

AFRL-ML-WP-TR-2000-4127

**STUDY OF NOISE AND DEFECT LEVELS IN
INFRARED CADMIUM MERCURY
TELLURIDE**



**FLORIDA INTERNATIONAL UNIVERSITY
10555 W FLAGLER ST
MIAMI FL 33174**

September 2000

Final Report for: 4/12/96 -- 7/12/99

Approved for public release; distribution unlimited.

**Materials and Manufacturing Directorate
Air Force Research Laboratory
Air Force Materiel Command
Wright-Patterson AFB, OH 45433-7750**

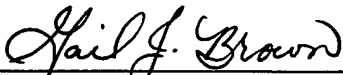
20001127 079

NOTICE

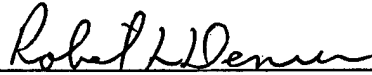
USING GOVERNMENT DRAWINGS, SPECIFICATIONS, OR OTHER DATA INCLUDED IN THIS DOCUMENT FOR ANY PURPOSE OTHER THAN GOVERNMENT PROCUREMENT DOES NOT IN ANY WAY OBLIGATE THE US GOVERNMENT. THE FACT THAT THE GOVERNMENT FORMULATED OR SUPPLIED THE DRAWINGS, SPECIFICATIONS, OR OTHER DATA DOES NOT LICENSE THE HOLDER OR ANY OTHER PERSON OR CORPORATION; OR CONVEY ANY RIGHTS OR PERMISSION TO MANUFACTURE, USE, OR SELL ANY PATENTED INVENTION THAT MAY RELATE TO THEM.

THIS REPORT IS RELEASABLE TO THE NATIONAL TECHNICAL INFORMATION SERVICE (NTIS). AT NTIS, IT WILL BE AVAILABLE TO THE GENERAL PUBLIC, INCLUDING FOREIGN NATIONS.

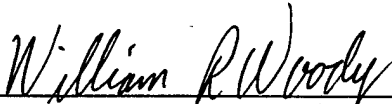
THIS TECHNICAL REPORT HAS BEEN REVIEWED AND IS APPROVED FOR PUBLICATION.



GAIL J. BROWN, Project Engineer
Sensor Materials Branch
Survivability & Sensor Materials Division



ROBERT L. DENISON, Chief
Sensor Materials Branch
Survivability & Sensor Materials Division



WILLIAM R. WOODY, Chief
Survivability & Sensor Materials Division
Materials & Manufacturing Directorate

Do not return copies of this report unless contractual obligations or notice on a specific document requires its return.

REPORT DOCUMENTATION PAGE

Form Approved
OMB No. 0704-0188

Public reporting burden for this collection of information is estimated to average 1 hour per response, including the time for reviewing instructions, searching existing data sources, gathering and maintaining the data needed, and completing and reviewing this collection of information. Send comments regarding this burden estimate or any other aspect of this collection of information, including suggestions for reducing this burden to Department of Defense, Washington Headquarters Services, Directorate for Information Operations and Reports (0704-0188), 1215 Jefferson Davis Highway, Suite 1204, Arlington, VA 22202-4302. Respondents should be aware that notwithstanding any other provision of law, no person shall be subject to any penalty for failing to comply with a collection of information if it does not display a currently valid OMB control number. PLEASE DO NOT RETURN YOUR FORM TO THE ABOVE ADDRESS.

1. REPORT DATE (DD-MM-YYYY)		2. REPORT TYPE Final Report		3. DATES COVERED (From - To) 12 Apr 1996 to 12 July 1999	
4. TITLE AND SUBTITLE Study of Noise and Defect Levels in Infrared Cadmium Mercury Telluride				5a. CONTRACT NUMBER F33615-96-C-5452	
				5b. GRANT NUMBER	
				5c. PROGRAM ELEMENT NUMBER 62102F	
6. AUTHOR(S) Dr. Carolyne M. Van Vliet Dr. Sylvia Mergui				5d. PROJECT NUMBER 4348	
				5e. TASK NUMBER 72	
				5f. WORK UNIT NUMBER 02	
7. PERFORMING ORGANIZATION NAME(S) AND ADDRESS(ES) Florida International Univ. 10555 W. Flagler Street Miami, FL 33174				8. PERFORMING ORGANIZATION REPORT NUMBER FIU001Z	
9. SPONSORING / MONITORING AGENCY NAME(S) AND ADDRESS(ES) MATERIALS & MANUFACTURING DIRECTORATE Air Force Research Laboratory Air Force Materiel Command WPAFB, OH 45433-7750. POC: GAIL J. BROWN				10. SPONSOR/MONITOR'S ACRONYM(S) AFRL/MLPO	
				11. SPONSOR/MONITOR'S REPORT NUMBER(S) AFRL-ML-WP-TR-2000-4127	
12. DISTRIBUTION / AVAILABILITY STATEMENT Approved for Public Release. Distribution Unlimited.					
13. SUPPLEMENTARY NOTES This is a Historically Black College or University (HBCU) Final Report					
14. ABSTRACT The objective this HBCU program was to measure the different types of signal noise in mercury cadmium telluride (MCT) materials, and to correlate the type and magnitude of the noise to measured defect levels in the same samples. This type of study had been previously been done for thick MCT layers grown by liquid phase epitaxy decades ago. This program was to look at the more advanced epitaxial MCT layers grown by molecular beam epitaxy. Samples were measured with a Noise Spectrum Analyzer down to cryogenic temperatures and by a Photo-Induced Current Spectroscopy Technique. Results of these measurements showed that the 1/f noise in the MCT epitaxial samples was indicative of interface states between the epilayer and the substrate, and not due to alloy fluctuations in the epilayer.					
15. SUBJECT TERMS Infrared Materials, Cadmium Mercury Telluride, Noise, Defect Levels					
16. SECURITY CLASSIFICATION OF:			17. LIMITATION OF ABSTRACT SAR	18. NUMBER OF PAGES 29	19a. NAME OF RESPONSIBLE PERSON Dr. Gail J. Brown
a. REPORT U	b. ABSTRACT U	c. THIS PAGE U			19b. TELEPHONE NUMBER (include area code) 937 255-4474 X3238

Standard Form 298 (Rev. 8-98)
Prescribed by ANSI Std. Z39.18

STUDY OF NOISE AND DEFECT LEVELS IN
INFRARED CADMIUM MERCURY TELLURIDE

CAROLYNE M. VAN VLIET
SYVIA MERGUI

FLORIDA INTERNATIONAL UNIVERSITY
10555 W. FLAGLER STREET
MIAMI, FLORIDA 33174

AUGUST 2000

FINAL REPORT FOR 12 APRIL 1996 - 12 JULY 1999

MATERIALS AND MANUFACTURING DIRECTORATE
AIR FORCE RESEARCH LABORATORY
WRIGHT PATTERSON AFB OH

Table of Contents

- I. Introduction and Purpose of the Study
- II. Experimental Techniques Established under the Contract
 - 2.1 Installing the basic noise instrumentation, 1 Hz to 150 MHz.
 - 2.2 Automated algorithms developed.
 - 2.3 Measurement procedures.
 - 2.4 Processing techniques.
 - 2.5 Optical response techniques ("PICTS")
- III. Experimental Results
 - 3.1 Noise spectra of long wavelengths epilayers.
 - 3.2 Theory developed and interpretation.
 - 3.3 References.
- IV. Theses and Dissertations
 - 4.1 Theses under this contract.
 - 4.2 Associated theses and dissertations.
- V. Publications under this contract
- VI. Relation with FAST Center, supported by AF-OSR
- VII. Conclusions
- VIII. Appendices
 - 8.1 Patents.
 - 8.2 Spending curve.
 - 8.3 Property acquired under this contract.

I. Introduction and Purpose of the Study.

Cadmium Mercury Telluride ($\text{Cd}_x \text{Hg}_{1-x} \text{Te}$) is an important highly sensitive infrared detector. For $0.15 < x \leq 0.23$ the mixed II-VI compound provides narrow band semiconductors which can easily be optically excited, providing cut-off wavelength between $5\mu\text{m}$ and $20\mu\text{m}$. For $x < 0.15$ the material is a semimetal with no band gap. The samples studied by us, grown by MBE techniques at Rockwell Semiconductors had cutoff wavelengths at 80 K of $10.5\mu\text{m}$ and $12\mu\text{m}$, corresponding to intrinsic bandgaps of 114.3 meV and 103.3 meV, the composition parameter x being 0.219 and 0.211, respectively. The samples investigated were epilayers of $\sim 10\mu\text{m}$ thickness (after re-etching), deposited on a semi-insulating substrate of CdTe.

Sensitive infrared photodetectors are useful only insofar the electrical noise in excess of Johnson noise, i.e., generation-recombination noise and flicker ($1/f$) noise, is low. Originally it was believed that an "ideal" detector, excited by an rf modulated optical signal should have a signal to noise ratio at the output, measured e.g., as a Norton generator of the output current signal and current noise, equal to the signal to noise ratio of the incident photon flux; this would indicate that the detector only shows *photo-induced noise*. However, in the fifties and sixties the author (P.I.) showed that photoinduced noise is part of the statistical process known as *generation-recombination noise*. If there are no traps or specific recombination centers and if Auger processes are absent, the recombination process will add an amount of noise equal to that of the generation process of photocarriers, so that the minimum amount of g-r noise is twice the photo-induced noise. Thus, in such an "ideal" detector we have

$$\left(\frac{S}{N} \right)_{\text{photon}}^* \equiv \frac{i(\nu, f)}{[2 G_{i,ph}(\nu, f) \Delta f]^{1/2}} = \frac{1}{\sqrt{2}} \left(\frac{S}{N} \right)_{\text{photon}} \quad (1.1)$$

Here i is the photosignal of optical frequency ν and electrical (information) frequency f , G_i is the electrical noise at the output with bandwidth $\Delta f \ll f$, and the $*$ indicates that the detector is *photonlimited*, i.e. the photocarriers recombine with the radiative lifetime which can be theoretically computed, see [1],[2].

The *spectral noise equivalent power* (SNEP) is defined as the signal referred to at the input, for which (S/N) at the output equals unity. Hence,

$$\begin{aligned} P_{eq}(\nu, f; \Delta f, A) &= h\nu J_{eq}(\nu, f; \Delta f, A) \\ &= h\nu [G_{i, \det}(f) \Delta f]^{1/2} / R_i(\nu, f); \end{aligned} \quad (1.2)$$

here $J_{eq}(\nu, f; \Delta f, A)$ is the photon noise incident on a detector of area A optical frequency ν and information bandwidth $(f - \frac{1}{2}\Delta f, f + \frac{1}{2}\Delta f)$, while $R_i(\nu, t)$ is the current responsivity. Taking $\Delta f = 1\text{Hz}$ and $A = 1\text{ cm}^2$ we define the *detectivity* more specifically as the reciprocal spectral noise equivalent power,

$$D_\lambda(\nu, f) = 1 / P_{eq}(\nu, f; 1, 1). \quad (1.3)$$

The units are $(\text{Watt})^{-1} \text{ cm}(\text{sec})^{-1/2}$. The subscript λ indicates that we are interested in the sensitivity for a line source (such as a laser) of nearly fixed wavelength $\lambda = c/\nu$. If the noise is photonlimited - i.e., the output noise is no more than twice the photo-induced noise - the detectivity is denoted by $D_\lambda^*(\nu, f)$. Computations for various line sources are found in [1].

Another situation may occur if the detector sees black body radiation noise of temperature $T > T_0$ (detector) in a solid angle $\Omega=2\pi$, while the detector's cutoff frequency is ν_0 ; we now indicate the detectivity by

$$D_T(\nu_0, f) = 1/P_{eq}(\nu_0, f; 1, 1); \quad (1.4)$$

for the photon-limited case the detectivity is again denoted as $D_T^*(\nu_0, f)$. Nomographs for D_T^* at frequencies $f \ll 1/\tau_{\text{radiative}}$ are given in [1]. For a detector like Cd Hg Te, with cutoff frequencies of order $10\mu\text{m}$ and seeing black body radiation of 300 K, the theoretical detection limit $D_{(300)}^*$ would be $5 \times 10^{10} \text{ watt}^{-1} \text{ cm s}^{-1/2}$. Experimentally observed detectivities are usually no larger than 10^9 .

Under the present contract we have not been able to determine either D_λ^* or D_T^* , since we had no means to determine the absolute responsivity, necessary to determine the equivalent input noise from the measured output noise; in particular, we had no power-calibrated line source or standard blackbody source. However, our primary purpose was to investigate the detector output noise, either as a Norton generator $(G_i(f)\Delta f)^{1/2}$, or as a Thevenin generator $(G_v(f)\Delta f)^{1/2}$ in series with the DUT ("device under test"). To avoid ambient photo-induced noise the samples were surrounded by a radiation shield, kept at detector temperature T_0 . Thus, the samples were in thermal equilibrium, except for the small current i necessary to detect the conductivity fluctuations $\Delta\sigma$ associated with generation-recombination (g-r) noise. The samples were investigated in the range 300-50K. From the resistance versus $1000/T$ plots, it was clear that the samples were mainly intrinsic (300-100K), being extrinsic only below 100K. Yet, noise due to intrinsic transitions, taking place most likely via Shockley-Read-Hall (SRH) generation-recombination centers, was never observed, i.e., not discernable above the naturally present thermal noise. The noise was therefore due to defect levels.

The main purpose of this study was therefore to determine the origin and nature of these defect levels and to assess their magnitude quantitatively by comparing with the appropriate theoretical expressions for trapping g-r noise. One or two Lorentzians,

$$G_i(f) = \sum_i A_i \tau_i / (1 + \omega^2 \tau_i^2) \quad (1.5)$$

were observed in all measured samples. In addition, $1/f^\alpha$ noise, $1 \square \propto \square 1.145$, was always present.

The results have been laid down in the M.S. thesis of Nichols Paul (December, 1997) and in two journal papers. This is described in parts III, IV, and V. N.B. In the sections that follow the noise spectral densities are denoted by $S_i(f)$ or $S_v(f)$; the symbol "G" was only used in this section, since "S" was used for signal.

II. Experimental Techniques Established under the Contract.

2.1 *Installing the basic noise instrumentation in the range 1 Hz to 150 MHz.*

At the onset of this contract, there was some general equipment (digital voltmeters, oscilloscope, helium flow cryostat by Janis, etc.) but no specific noise-measuring set-up. We started from "scratch", first in a small part of an already occupied room in the old Engineering Building, ECS 137, later in a specifically designed new space in the present Center for Engineering and Applied Sciences, EAS 3810. We are greatly indebted to Prof. Gustavo Roig, Associate Dean and then Acting Chair, for pushing through this project. The current laboratory is approximately 800 sq. ft. of space. Central to it is a shielded Faraday cage of 8' x 10', having a doubly shielded copper sheet solder-connected wall, permitting a RF pick-up attenuation of 140 dB; it also has a line filter with isolation-interrupter for incoming power, so that virtually no stations on the main line come inside.

The cage has a special and separate external ground. The laboratory has also a sample-preparation site, electronic components work benches (4), and two computers connected to the University's Unix. In addition, there are three desks for graduate students.

The main instrumentation in the Faraday cage consists of a HP 3589A Network/Spectrum Analyzer, a Brookdeal (Princeton Applied Research) 5184 Preamplifier, with internal noise of less than $0.8 \text{ nV} / \sqrt{\text{Hz}}$ noise at 10 Hz, a Quatech 1 Hz-100kHz white noise generator, a self-built 100 kHz-10 MHz avalanche diode + op.amp white noise generator, a brass box (1/4" walls) input circuitry container, a Janis Helium flow cryostat allowing temperatures from 400 K down to 10K*, a Cryotronics temperature monitoring system*, and a data-processing and postaveraging computer connected to a four-color printer. All items, except those marked by *, were purchased under the Wright-Laboratory AF contract. The detailed operation of each part is discussed in depth in the M.S. thesis of Nichols Paul, our first graduate to base his research on the premises of the presently discussed grant. Copies of the thesis were sent to the Air Force in 1998. We will here be brief in our description. The overall flow diagram of the measurement procedure is given in Fig. 1.

The front-end, inside the specially constructed brass box contains the biasing circuitry for the DUT (device under test). For room temperature the crystal holder with the device can be inside the box, see Fig. 2; at other temperatures the DUT is on the cold finger of the Janis cryostat, which is connected to the external port by a mini coax cable (1mm cross section) of 50Ω , and from the external port to the brass box via a regular coaxial cable of 50Ω . Extreme care was taken to avoid "multiple grounding". The noise generator signal also entered the brass box, being in series with a 4K load, thus providing a Norton generator $V_n/4K$.

The equivalent circuit, showing the current generators provided by the DUT (i_{xN}), the load impedance (i_{LN}), and the noise-signal generator (i_{sN}), as well as the voltage and current sources representing the Brookdeal amplifier (V_{aN} and i_{aN} , respectively), are shown in Fig. 3.

The HP analyzer was used in the fast-fourier-transform mode (FFT) for spectral frequencies from 1 Hz to 100 KHz. For higher frequencies the swept-spectrum mode (SPM) was employed, being based on variable 18 dB/octave digital filters, local oscillators and multiple heterodyning. Generally, we utilized the SPM from 50 KHz - 4MHz (switching white noise generators at 100 KHz). Since the local oscillators are swept linearly, this HP analyzer had the disadvantage that the frequency scale was linear, while the noise output in $\text{dBm}/\sqrt{\text{Hz}}$ was basically a logarithmic scale. The view of the spectrum as displayed by the analyzer was therefore "semilog", i.e., log (magnitude) vs. linear frequency. HP assured us that it was not possible to construct this instrument with a log (frequency) scale. For this reason, analog measurements, as in the SPM mode of this analyzer, are virtually never reported these days and MOST investigators do not go beyond 100 kHz, which is the range limit for FTT's, which generally have a "log-log" display. This is a pitfall of modern-day techniques! The author employed already in 1954 a (non-automated) point by point analyzer which gave accurate absolute data ($\pm 5\%$ error) from 1Hz to 10MHz. Often, very valuable information occurs at the high frequency end of the spectrum! The HP 3589A allows one to go up to 150 MHz, but a *conversion scheme* is necessary.

Therefore, see Fig. 1, the interface output of the HP analyzer was connected to a 133 MHz Pentium

computer, with a three-fold purpose. (1) The computer collected data for some 40 "logarithmically evenly-spaced" frequencies for 0.5 to 2 minutes per point in order to do *postaveraging*; i.e., we wanted to display jitter-free points (\square 5%) and not the "noisy" spectra, typically reported by most researchers today (my basic point being: why should automated data-acquisition in the nineties be less accurate and 'stable' than my 1954 point-by-point spectra?). (2) The computer prepared a spreadsheet for the acquired data, which typically entail three measurements at each frequency. (3) The computer formats the data with equal decade-spacings for abscissa and ordinate, so that the log-log display of say a $1/f$ spectrum, appears as a -45° slope, while a Lorentzian falls off with 6 dB/octave or a -63.44° slope. This is discussed more fully in the next subsection.

2.2 Automated algorithms developed.

The essential algorithmism were done within a Lab View program, once the data were transferred from the analyzer to the computer. The program was designed to take three measurements M_1, M_2, M_3 for the current-noise spectrum or two M_1, M_3 for the voltage-noise spectrum, - at the user-chosen frequencies and save the data to a spreadsheet file. Further processing is done by Microsoft Excel (although any spreadsheet software would suffice). Curve-fitting was accomplished by either Excel (visually) or using least-square fitting with Prism software available from Graphpad Co. All software programs were purchased with Grant funds. For a fit of $1/f$ noise and two Lorentzians, we obtained the best guess for α, A, B , and C in the equation

$$S(f) = \frac{A}{f^\alpha} + \frac{B}{1 + \omega^2 \tau_1^2} + \frac{C}{1 + \omega^2 \tau_2^2} \quad (2.1)$$

where $\omega = 2\pi f$. The data given later are obtained as

$$\sum_i [(experimental\ value - theoretical\ value)_i]^2 = \text{minimum} \quad (2.2)$$

The Lab View program, by National Instruments, Inc., is an object-oriented program. VIEW is an acronym for Virtual Instrument Engineering Workbench. LabView is powerful in that it uses simulated controls to operate and imitate real instruments. The controls are called virtual instruments (VTS) for this reason. The three parts of LabView VI are the front panel, the block diagram with icons for the desired VTS's, and the system controller. The Hewlett Packard General Purpose Interface Board (GPIB) acts as a medium between the computer and the data-based instrumentation devices, such as the spectrum analyzer. The controller allows data transfer to begin by releasing the attention signal (ATN) on the GPIB.

The devices on the GPIB all have numbered addresses that go from 0 to 30 on the chip. They include the address of the spectrum analyzer (#19), the Lakeshore temperature controller (#12), etc.

The various GPIB commands include: Interface Clear - resets, activity; Selected device clear - resets device modes; Trigger - starts operation; etc. The data acquisition program is designed so that the user has flexibility in taking a noise measurement. Automatic features in the program do not take precedence over user's control. E.g., the M_1, M_2 , and M_3 readings may be taken over an individual frequency at a time, or over a range of frequencies in advance. Parameters within the program, such as the calibration voltage V_n from the noise generator, or the series resistance R_s employed in the measurement, may be adjusted during the run of the program prior to obtaining final data, which are sent to a Canon BJC620 bubblejet printer.

2.3 Measurement procedures.

Many present-day publications on noise are not reliable as to the magnitude reported. Most investigators simply use the dB read-out of their FFT analyzer, account for the gain of the preamplifier and thus compute the noise of the device, subtracting perhaps the amplifier noise as given by the manufacturer.

One fares slightly better by using the Johnson noise of the input resistance, R_{DUT}/R_{LOAD} , as a calibration standard. In that case, let M_1 be the reading with the DUT "activated" (i.e. current through it to obtain the conductance fluctuations noise) and M_3 the reading with no current through the DUT. Then, assuming R_{DUT} to be constant (i.e., the I-V characteristic is linear), $M_1 - M_3$ refers to the excess noise: the noise of the DUT minus its thermal noise. Thus we have for the excess noise:

$$S_V(f) = \frac{M_1 - M_3}{M_3} \times R_{In} \times 1.7 \times 10^{-17} V^2 / \text{Hz} \quad (2.3)$$

where R_{In} is the value of the input resistance, R_{DUT}/R_L , in kilo Ohms and the temperature of R_{In} is supposed to be 300 K. The problem with this procedure is that: a) R_{DUT} and R_L may be at different temperatures; b) There may be a shunting input capacitance (in particular if a rather long coax cable to the cryostat is used) so that there is an R-C roll-off at high frequencies, which may be mistakenly interpreted as a device-Lorentzian component. This pitfall leading to a false interpretation of contact noise in resistors by Campbell and Chipmann, was already uncovered by the author and coworkers in 1954 [3]. Therefore, my noise groups, as well as those of colleagues Bosman at the University of Florida [4] and of Zijlstra at the University of Utrecht [5], have always made it a point to determine the noise current spectra $S_i(f)$, rather than the noise voltage spectra, employing a three-point procedure in which the input impedance, $Z_{In} = R_{In}/(1 + j\omega C_{In}R_{In})$, cancels out.

Thus, let

- M_1 be the analyzer's output reading with current through the DUT;
- M_2 be the analyzer's output reading with no current through the DUT and with a noise signal generator voltage V_n applied over a small resistor in series with R_g ;
- M_3 be the analyzer's output reading with no current through the DUT and noise generator off;

Then we clearly have for the excess current noise (i.e., over and above the thermal noise of the DUT):

$$S_i(f) = \frac{M_1 - M_3}{M_2 - M_3} \frac{V_n^2}{R_g^2} A^2 / \text{Hz} \quad (2.4)$$

In case the I-V characteristic is not strictly linear, a correction must be made to M_3 or, a fully accurate four or five-point method must be used. For our samples the I-V characteristics were always linear. In the earlier measurement procedure we employed (2.3), since R_{DUT} was usually not affected by capacitive roll-off. In the later, most accurate data we employed (2.4); the computation was done by the data-acquisition computer program, discussed in the previous subsection.

2.4 Processing Techniques.

Although the five samples sent to us by Dr. Gail Brown were shiny and pre-etched, we generally

etched them once more in a standard solution of bromine and methanol, removing 1 to 1.5 microns of the epilayers. After that we defined an active region of approximately 2mm^2 using a mask and we evaporated indium contacts at both ends of the epilayer front surface. Better contacts (less contact $1/f$ noise) might have been obtained by soldering indium to the epilayer. However, since that method is risky and we had too few samples, that method was abandoned.

Various *crystal holders* were constructed. Silverpasted leads were abandoned in favor of strong phosphor-bronze springs at each indium covered end; these connections proved to be noise-free (as in past applications by the author).

The characteristics of the two principal samples used in our studies are listed in the two tables below:

Table 1.

Sample	65K	80K
2-344	12.7	12.0
2-348	11.0	10.5

Layer	Band	Base layer composition x	Layer thickness in Hall (μm)	77K carrier conc. $\times 10^{14}(\text{cm}^{-3})$	77K mobility $\times 1000 (\text{cm}^2/\text{Vs})$
2-344	VLWIR	0.211	14.0	4.8	195
2-348	VLWIR	0.219	13.3	5.4	160

2.5 Optical response techniques ("PICTS").

Photo-Induced Current Transient Spectroscopy is another method to determine energy positions and number of defects present in a material - if the right conditions prevail. The method is similar to DLTS (Deep-Level Transient Spectroscopy), but no Schottky-barrier contact is required to start a pulse response. The FAST Center of FIU (supported by AF-OSR) has an elaborate and fully automated measurement system from Biorad, DL8000 for either DLTS or PICTS. In the latter case the sample is irradiated with ambient light. A rather strong source is required to override the large dark conductivity (with radiation shield) of our samples. Illuminations with an incandescent source filtered by an acquired simple grating monochromator appeared to be too weak and not acceptable to the software of the system. Only illumination with the built-in laser of the system gave a measurable response. The photocarriers so produced (laser wavelength 750 nm) had a high absorption coefficient. An example of a photocurrent decay is given in Fig. 4. The decay times were found to be very long (under 50 ms) and near independent of temperature. We attribute therefore the photo-induced current decay as caused by tunneling to interface states, a temperature-independent process. The life times so observed do not correspond to any of the generation-recombination Lorentzians, but rather to the quite high $1/f$ noise observed in the spectra. We note

hereby that tunnel processes form the oldest, reasonable, explanation of inherent $1/f$ noise, as described in McWhorter's 1955 Ph.D. thesis [6]. New PICTS measurements are planned, using a powerful infrared source, upon modification of the machine's software commands.

III. Experimental Results

3.1 Noise spectra of long wavelength epilayers.

In Fig. 5 we represent the resistance vs. $1000/T$ for sample 2-344. The behavior is intrinsic down to about 40K. The I-V characteristic was strictly linear, indicating ohmic behavior, see Fig. 6. Typical noise spectra for $T = 300K$ and $T = 100K$ are given in Figs. 7 and 8. In both figures two Lorentzians are discernable.

The data are summarized in Table II.

Table II.

T [K]	A [V ² /Hz]	α [number]	B [V ² /Hz]	τ_1 [sec]	C [V ² /Hz]	τ_2 [sec]
300	6.121e-11	1.083	2.178e-15	7.644e-6	4.026e-16	4.243e-7
150	3.405e-9	1.323	2.095e-15	4.145e-6	-	-
100	2.737e-9	1.100	1.951e-13	1.373e-5	1.615e-14	7.732e-7

No detailed analysis has been made of these data.

It can be seen, however, that the time constant increases only very little (a factor ~ 2) from 300K to 100K. Both defect levels are therefore very shallow, probably of order 10-5 meV.

More details are available for sample 2-348. We reproduce here some data reported in the Journal of Applied Physics (15 June 1999), together with a possible interpretation (section 3.2) below. The resistance vs. $1000/T$ is given in Fig. 9. Clearly the sample is intrinsic down to 100K, below which it becomes n-type due to the donor doping of $5.4 \times 10^{14} \text{ cm}^{-3}$.

Noise spectra for 300K, 100K and 50K are given in Figs. 10, 11, and 12, respectively.

Notice that for Fig. 11 the three-point method was used. The Johnson noise and amplifier noise (in A^2/Hz) are also shown. The data are summarized in Table III.

Table III.

T [K]	A [A ² /Hz]	α	B [A ² /Hz]	τ [s]
300	1.348×10^{-15}	1.000	1.401×10^{-20}	6.474×10^{-7}
200	5.045×10^{-15}	1.13	3.338×10^{-21}	5.62×10^{-7}
100	6.460×10^{-16}	1.184	5.240×10^{-21}	1.744×10^{-6}
50	1.830×10^{-16}	1.145	5.312×10^{-22}	1.587×10^{-6}

The plot of $\log \tau$ vs $1000/T$ is given in Fig. 13. The dashed line gives a single slope of 12 meV; the full drawn line with a slope of 20 meV and a plateau at temperatures below 100K is more realistic and will be used in the interpretation of Section 3.2 below.

3.2 Theory developed and interpretation.

If the $1/f$ noise were due to bulk fluctuations, Hooge's law would apply [6].

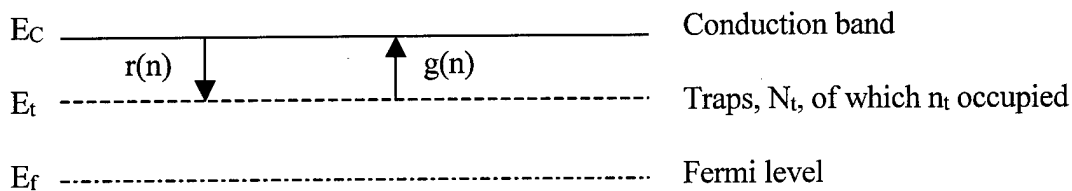
$$S_I(f) = \alpha_H I_o^2 N_o / f \quad (3.1)$$

where $N_o = n_o A d$ is the total number of free electrons in the epilayer. With $N_o = 5.26 \times 10^{10}$ at 100K, this would yield a very high Hooge parameter, $\alpha_H = 0.15$. Since any value $\geq 10^{-3}$ is unlikely, the $1/f$ noise clearly does not represent a bulk phenomenon described by (3.1). Rather, the $1/f$ noise is indicative for interface states between the epilayer and the substrate, in harmony with the interpretation of the PICTS data.

We now discuss the generation-recombination noise. Since the time constants vary only weakly with temperature, intrinsic transitions noise is clearly absent. Noise due to extrinsic transitions from the donors to the conduction band is likewise unlikely, since in the temperature range concerned no noticeable freeze-out of the donors occurs. We must therefore attribute the g-r noise to trapping, i.e., there are shallow electron traps below the induction band, or shallow hole traps above the valence band. Starting with the former, we have

$$S_I(f) = I_o^2 S_n(f) / n_o^2 \quad (3.2)$$

where $S_n(f)$ is the spectral density of the variance $\langle \Delta n^2 \rangle$. (Basically, we need *total* numbers, N_o , rather than n_o , unless for simplicity we assume the volume to be 1 cm^3 .) The diagram for the transitions involving shallow traps is given below. Noise from shall traps is described in various places [7-9].



Let N_t be the number of traps, n_t its stochastic occupancy, and n_{t0} its equilibrium occupancy; likewise, let n denote the conduction band carriers and n_0 the equilibrium value. The instantaneous generation and recombination rates are

$$g(n) = \gamma n_t \equiv \delta n_l n_t, \quad (3.3)$$

$$r(n) = \delta n(N_t - n_t); \quad (3.4)$$

Here n_l is the Shockley-Read "would-be" quantity: the number of carriers that would be in the conduction band if the Fermi level coincided with the trap level; further, $\delta = \sigma_t \langle v_n \rangle$ where σ_t is the trap capture cross section and $\langle v_n \rangle$ the mean thermal velocity of the free carriers. From detailed balance we have

$$n_l n_{t0} = n_0(N_t - n_{t0}). \quad (3.5)$$

Now if N_l is the total "donors-minus-acceptors excess" at $T = 0K$, we have in addition the neutrality constraint

$$n + n_t = N_l \quad (3.6)$$

and, *a fortiori* in equilibrium.

$$n_0 + n_{t0} = N_l. \quad (3.7)$$

Carriers are therefore distributed over the conduction band and the traps. According to g-r noise theory, the effective lifetime and variance are

$$\tau = \frac{1}{r'(n_0) - g'(n_0)}, \quad (3.8)$$

$$\langle \Delta n^2 \rangle = \frac{g(n_0)}{r'(n_0) - g'(n_0)} = \frac{r(n_0)}{r'(n_0) - g'(n_0)} \quad (3.9)$$

where $r' = dr/dn$, $g' = dg/dn$. From (3.3), (3.4), (3.6), (3.8), and (3.9) one easily finds

$$\tau = \frac{1}{\sigma_t \langle v_n \rangle (N_t - n_{t0} + n_0 + n_l)} \quad (3.10)$$

$$\langle \Delta n^2 \rangle = \frac{n_0(N_t - n_{t0})}{N_t - n_{t0} + n_0 + n_l} \quad (3.11)$$

$$\alpha = \frac{\langle \Delta n^2 \rangle}{n_0} = \frac{N_t - n_{t0}}{N_t - n_{t0} + n_0 + n_l} \quad (3.12)$$

Here α is the relative variance, being 1 for Poissonian noise and always < 1 for a fermion gas. From (3.7) and (3.12) we can also obtain the alternate expression in terms of n_0 :

$$\alpha = \frac{(N_t - n_l + n_0)(N_t - n_0)}{(N_t - n_l + n_0)N_l + n_0(N_t - n_0)} \quad (3.13)$$

Starting with (3.10) and noting that for most temperatures $n_{t0} \ll N_t$ and $n_0 \ll n_l$ (traps above Fermi level), we have

$$\tau \approx 1/\sigma_t \langle v_n \rangle N_t + n_t = \begin{cases} 1/\sigma_t \langle v_n \rangle N_t \text{ (low } T) \\ 1/\sigma_t \langle v_n \rangle N_c g_1 e^{(E_t - E_c)} (T > 100K) \end{cases} \quad (3.14)$$

where g_1 reflects spin and/or valley degeneracy. The behavior (3.14) is as observed in Fig. 12, full line. For α the term $n_0(N_1 - n_0)$ in the denominator of (3.13) is usually negligible. Then we have approximately,

$$\langle \Delta n^2 \rangle \approx n_0(1 - n_0/N_1) = N_1 \mu(1 - \mu) \quad (3.15)$$

where $\mu = n_0/N_1$; i.e., the carriers are binomially distributed over the conduction band and the traps. For the spectrum we have from Fourier analysis, replacing n_0 by N_0 , the total number of carriers in the actual volume, and, likewise N_1 by \hat{N}_1 the total donor excess,

$$S_n(f) = 4 N_0(1 - N_0/\hat{N}_1) \frac{\tau}{1 + \omega^2 \tau^2}. \quad (3.16)$$

The current noise becomes, using (3.2)

$$S_I(\omega) = 4 \frac{I_0^2}{N_0} \left(1 - \frac{N_0}{\hat{N}_1} \right) \frac{\tau}{1 + \omega^2 \tau^2}. \quad (3.17)$$

This is the basic result. A similar expression applies *mutatis mutandis* for shallow hole traps below the Fermi level.

Returning to the data of sample 2-348 for 100K, with $I_0 = 15\text{mA}$, $1/N_0 = 19 \times 10^{-12}$, and $\tau = 1.74 \times 10^{-6}\text{s}$, the computed value for the plateau constant B would be $7.44 \times 10^{-21} \text{A}^2/\text{Hz}$ if α were unity. The observed value (see Table III) is $5.24 \times 10^{-21} \text{A}^2/\text{Hz}$. This implies $\alpha = 0.70$ or $N_0/\hat{N}_1 = 0.30$. With the already stated value for N_0 this yields $\hat{N}_1 = 1.75 \times 10^{11}$. Or, reverting to the density we have $N_1 = \hat{N}_1/Ad = 1.35 \times 10^{15} \text{cm}^{-3}$. The known donor density is $N_d = 5.4 \times 10^{14} \text{cm}^{-3}$. Neglecting possible counterdoping, we find that there are $8.1 \times 10^{14} \text{cm}^{-3}$ shallow charged traps. The capture cross section is found from the low T limiting value of τ . With an educated guess for the effective mass, $\langle v \rangle \approx 8.12 \times 10^7 \text{cm/s}$, we obtain $\sigma_t \approx 10^{-17} \text{cm}^2$.

The identification of the traps cannot be made without having access to the technology of the sample preparation so that various parameters can be altered or controlled. If the traps are electron traps they could be due to oxygen [10]. More likely, however, the traps are hole traps due to mercury vacancies: Hg is known to introduce acceptor-like traps (triple) with the lowest level being 15 meV above the valence band [11]. Such traps are likely to occur during crystal growth, despite the overpressure of Hg in the MBE process. Noise measurements under optical radiation could confirm this proposed analysis in more detail. However, no time was available for further measurements during the contract.

3.3 References

- [1] K. M. Van Vliet, *Applied Optics* **6**, 1145-1169 (1967).
- [2] P. W. Kruse, R. D. McGlauchlin, and R. B. McQuistan, *Elements of Infrared Technology*, Wiley N.Y. (1962).
- [3] K. M. Van Vliet, C. J. Van Leeuwen, J. Blok, and C. Ris, *Physica XX*, 481-496 (1954).

- [4] G. Bosman, Ph.D. Thesis, Univ. of Utrecht (1981).
- [5] F. Hofman, R. J. J. Zijlstra, and J. C. M. Henning, *Solid-State Electronics* **31**, 279 (1988).
- [6] A. L. McWhorter, Ph.D. Thesis, MIT Lincoln Lab. Technical Report No. 80 (1955).
- [7] K. M. Van Vliet and J. R. Fasset, in *Fluctuation Phenomena in Solids* (K. E. Burgess, Ed.) Acad. Press N.Y. (1965), pp 267-359.
- [8] A. van der Ziel, *Noise: Sources, Characterization, Measurements*, Prentice Hall, Englewood Cliffs N.Y. (1970), p 83 ff.
- [9] C. M. Van Vliet and G. L. Larkins, Jr., "Theory of Multiple Trapping Noise", to be submitted to Phys Rev. B.
- [10] M. Yoshikawa, S. Leda, K. Maruyama, and H. Takigawa, *J. Vac. Sci. Technol.* **A3**, 153 (1985).
- [11] C. E. Jones, K. James, J. Merz, R. Braunstein, M. Burd, M. Eetemadi, S. Hutton, and J. Drumheller, *J. Vac. Sci. Technol.* **A3**, 131 (1985).

IV. Theses and Dissertations

4.1 Theses under this contract

- a) *Nichols Paul*, "Study of Electrical Noise in the Range 10 Hz to 1 MHz in Cadmium Mercury Telluride Infrared Detectors," M.S. Thesis, Florida International University, December, 1997.
- b) *Rolando Silvano Duran*, "Giga and Tera Hertz Noise Under an Applied Bias in Mesoscopic and Ballistic Nanometer Degenerate Semiconductor Structures," M.S. Thesis, Florida International University, December, 1998.

4.2 Associated Theses and Dissertations

- a) Yuping Chen, "Investigation of Generation-Recombination Noise and Related Processes in Aluminum-Gallium Arsenide TEGFETS and Hall Structures With Quantum Wells," Ph.D. Dissertation, Florida International University, December, 1998.

V. Publications under this contract

- a) "Generation-recombination noise and photo-induced transient conductivity in epitaxial Cd Hg Te long wavelength infrared detectors," Nichols Paul, Carolyne M. Van Vliet, and Sylvia Mergui, *J. of Crystal Growth* **197**, 547-551 (1999).
- b) "Electrical fluctuations and photo-induced current transients in $\text{Cd}_x\text{Hg}_{1-x}\text{Te}$ long wavelength epilayers," Nichols Paul, Carolyne M. Van Vliet, and Sylvia Mergui, *Journal of Appl. Physics* **85**, 8287-8291 (15 June 1999).

VI. Relation with FAST Center, supported by AF-OSR.

Much of this research we have done in conjunction with the FAST Center, one of five pilot projects in "Future Aerospace Science Technology" involving microwave and cryogenic applications. the author is a Co-PI of this large project, sponsored by the Air Force Office of Scientific Research (AFOSR) for a seven year period, 1995-2002. Since the budget of the Wright Lab sponsored contract only provided funds for one graduate assistant (Nichols Paul from 1995-1997; Rolando Duran, 1998), we were fortunate that FAST sponsored another graduate assistant, Yuping Chen, who did many measurements on gallium arsenide-derived devices. Thus, the equipment purchased and developed under the Wright contract has been fruitfully used for other solid state and micro materials endeavors. For the next year (2000-2001) R. Duran plans to do noise studies on gallium nitride derived devices, currently much in vogue because of their extremely fast response and usefulness for millimeter waves. The equipment bought under this grant, together with general cryogenic and multipurpose equipment of FAST will therefore serve as the basis for his Ph.D. work.

While the grant has only led to limited results for Cd Hg Te, it has enabled us to firmly establish a noise-measurement laboratory at FIU. Current facilities allow us to measure up to 150 MHz; extended facilities up to 12 GHz are being planned.

VII. Conclusions.

Noise facilities, automated but with the reliability and accuracy of former conventional point by point spectral measurements, have been established and made fully operational.

The generation-recombination noise of four Cd Hg Te samples, in radiative equilibrium with their ambience, has been investigated. Two samples have been analyzed in detail. The location of shallow traps has been verified. Most likely, the trapping noise is caused by the lowest of the triple acceptor levels introduced by mercury vacancies. The density of these levels is low ($\sim 10^{14}/\text{cm}^3$) but is nevertheless causing noticeable excess noise. We propose that future specimen be prepared with a higher mercury over pressure in the MBE apparatus. Interface states cause (too) large $1/f$ noise. Probably a more gradual transition between epilayers and substrate should be planned.

Time was not available to determine quantitatively the detectivity, D_A or D_T , of these infrared detectors. A rough calculation indicates, however, that we are about a factor 50 away from the theoretical radiative detectivity D_T^* at 100K for a 12 μm cutoff infrared detector of these samples.

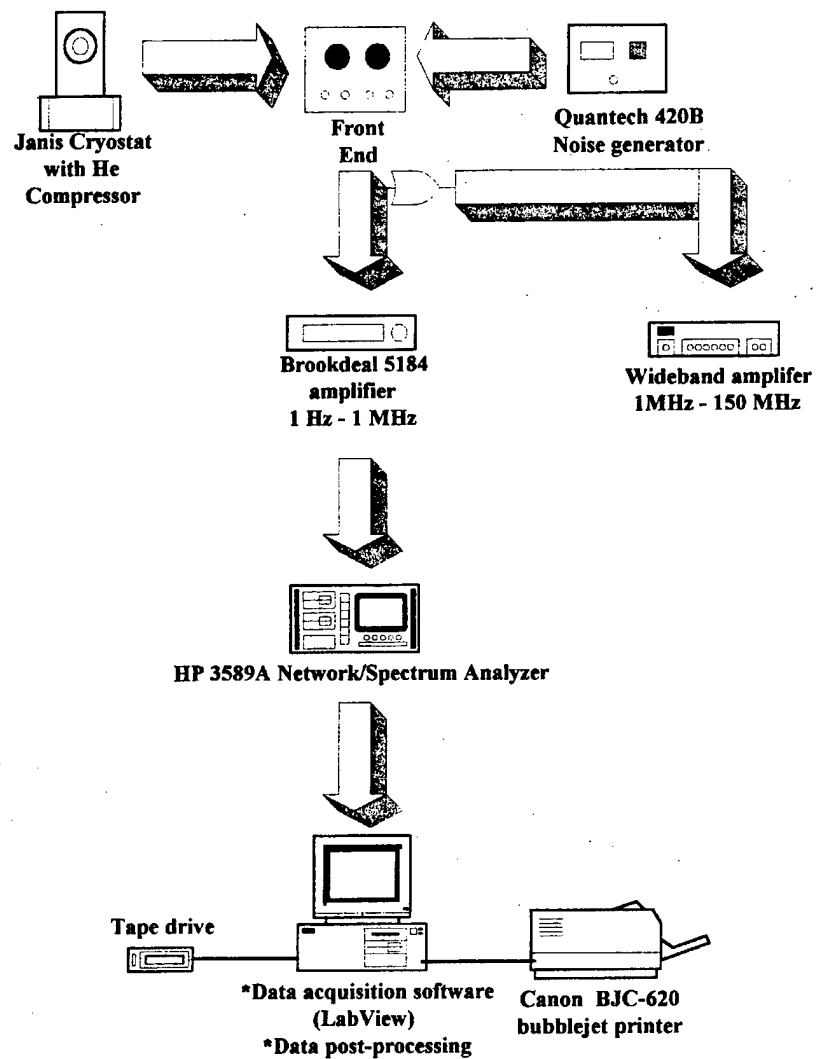
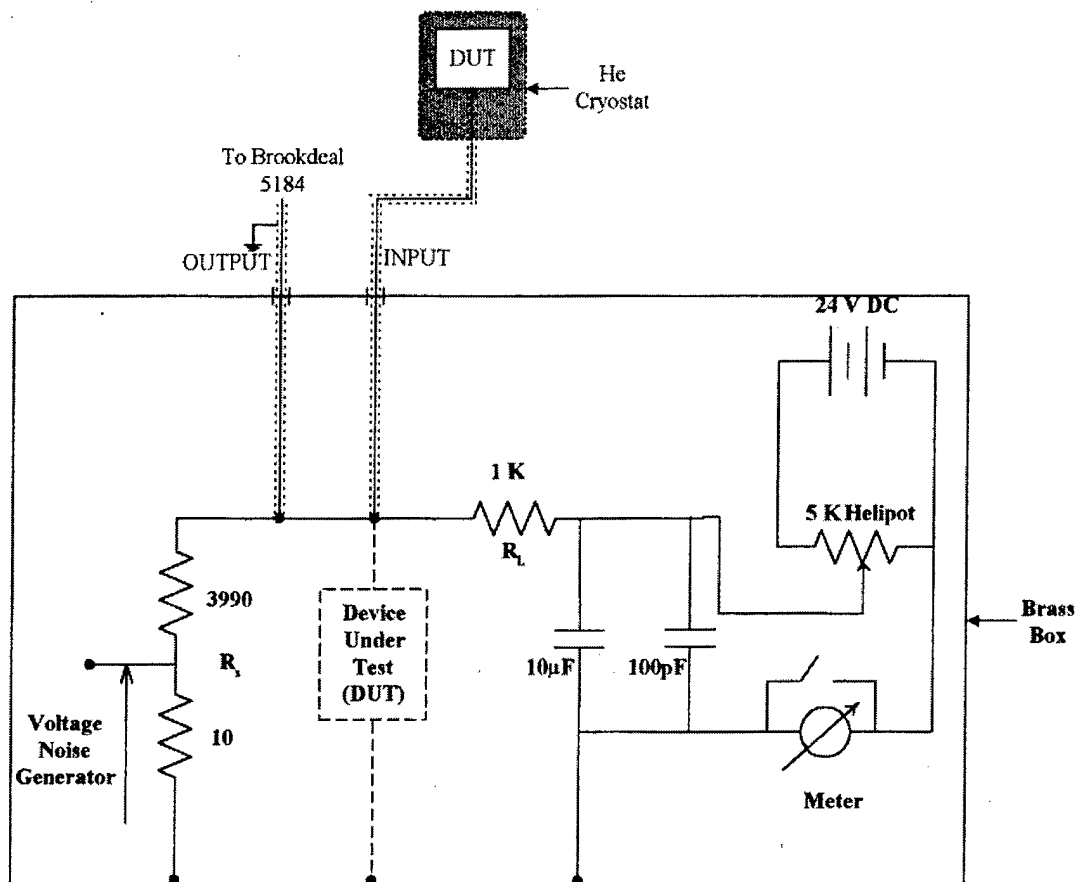


Figure 1. Flow diagram for measurement setup.



KEY:

- DUT in case no cryostat is needed
- coax cable, w/outer shield grounded
box is grounded to Brookdeal amplifier

Figure 2. Schematic diagram of biasing circuit.

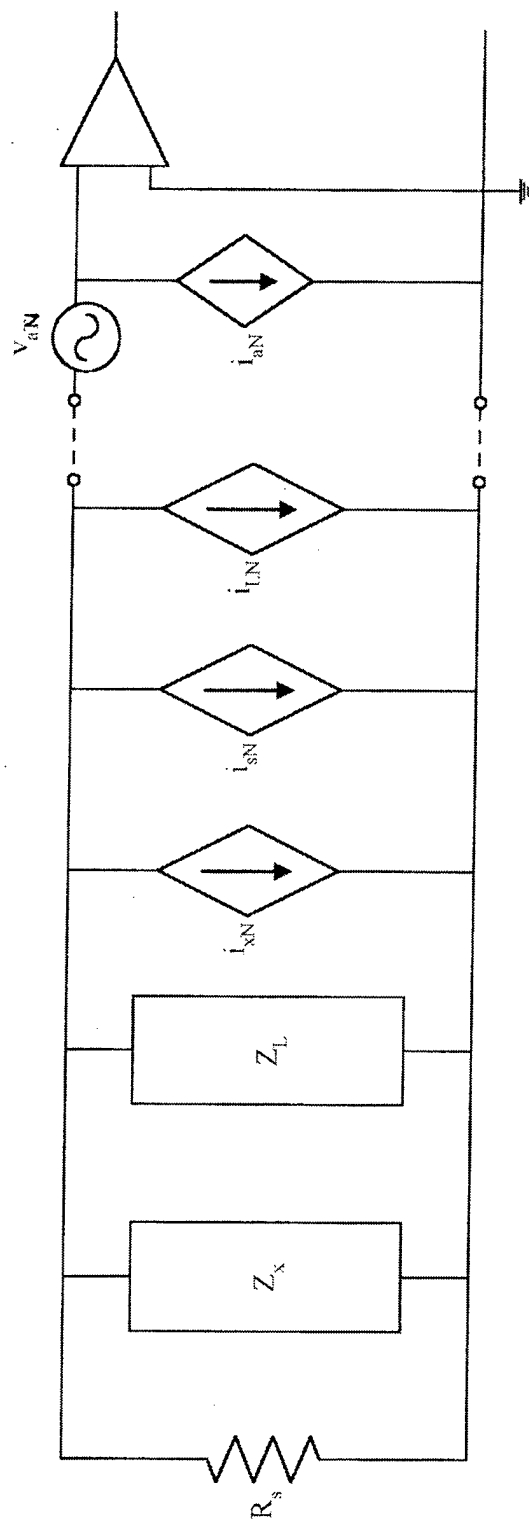


Figure 3. Equivalent circuit for Device Under Test

Figure 3. Equivalent Circuit for Device Under Test.

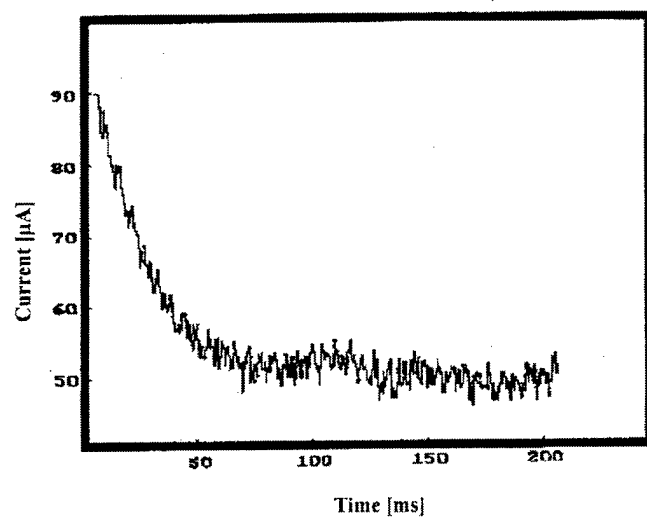


Figure 4. PICTS time response curve.

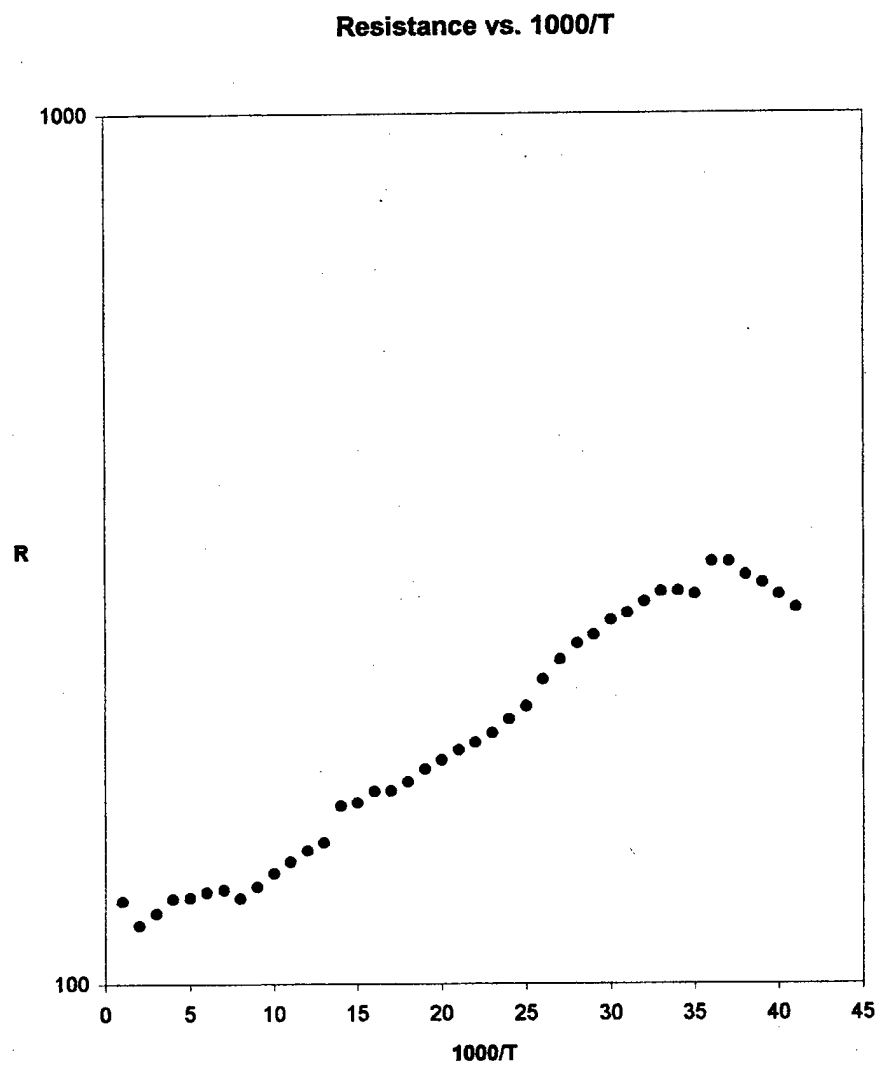


Figure 5. Resistance versus reciprocal temperature -Sample 2-344

I-V characteristic, sample 2-344

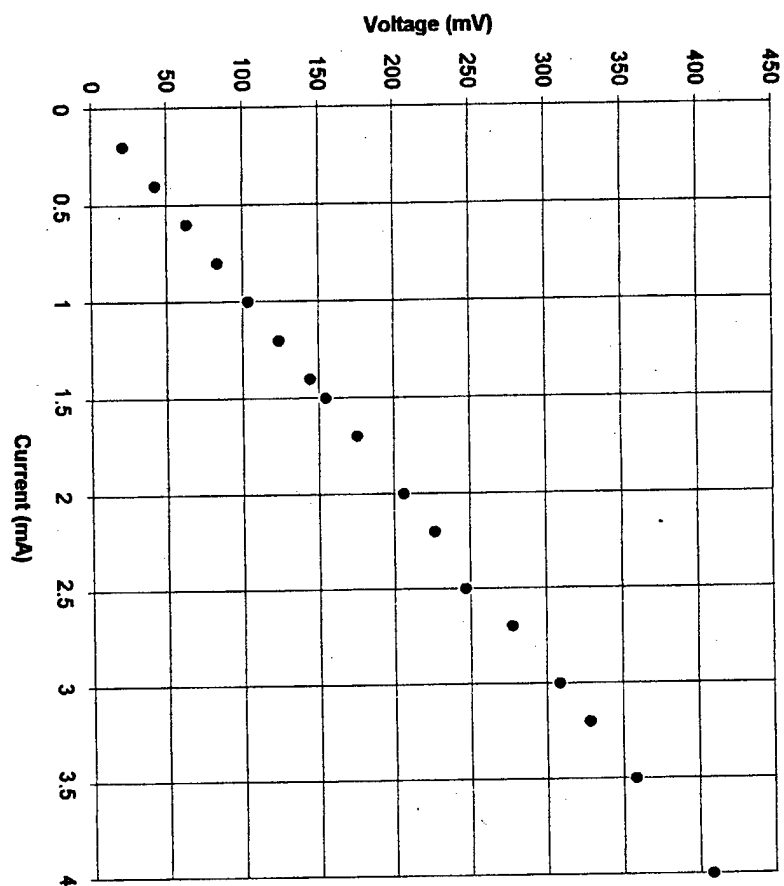


Figure 6.

Sample 2-344, T=300K

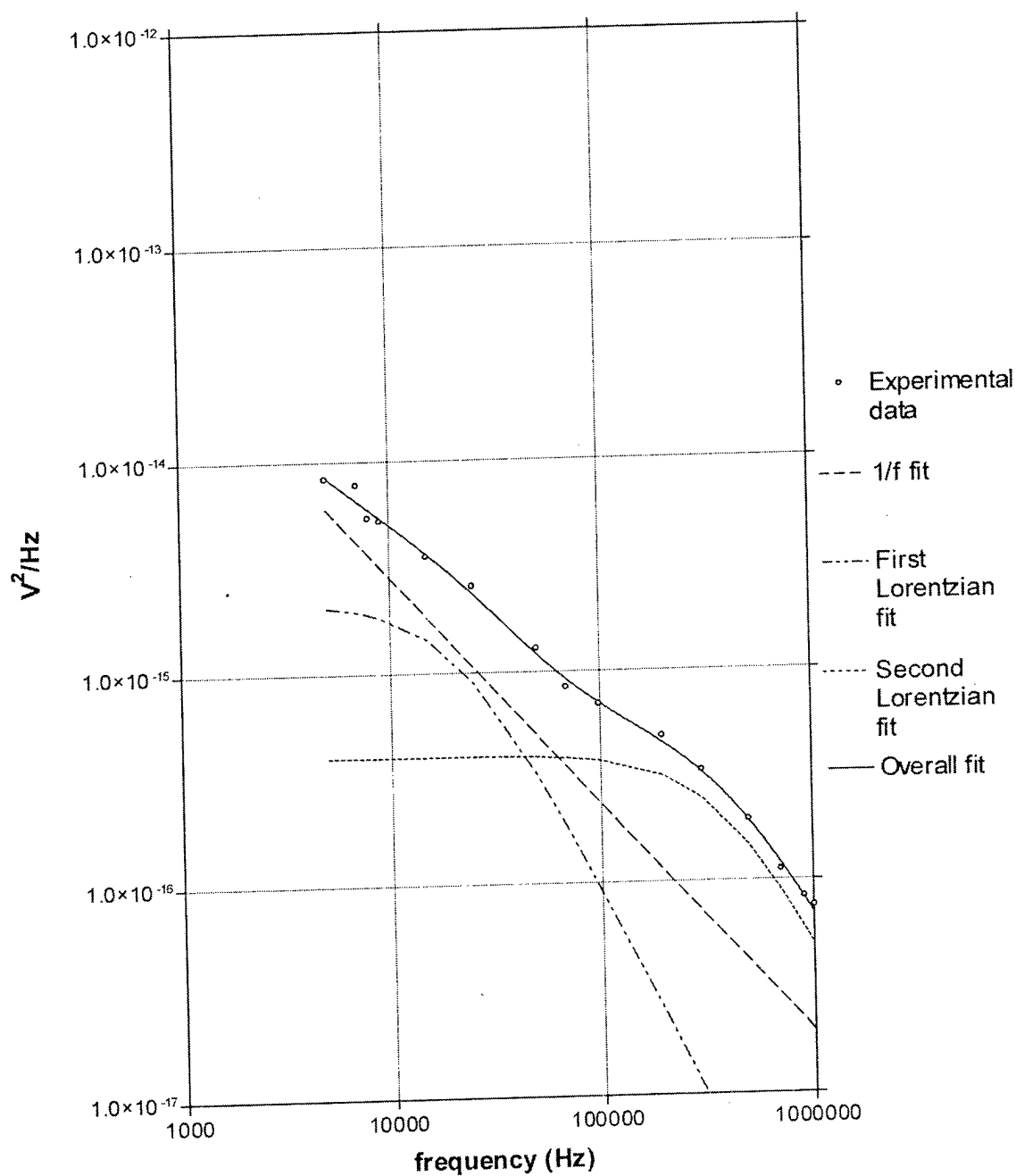


Figure 7.

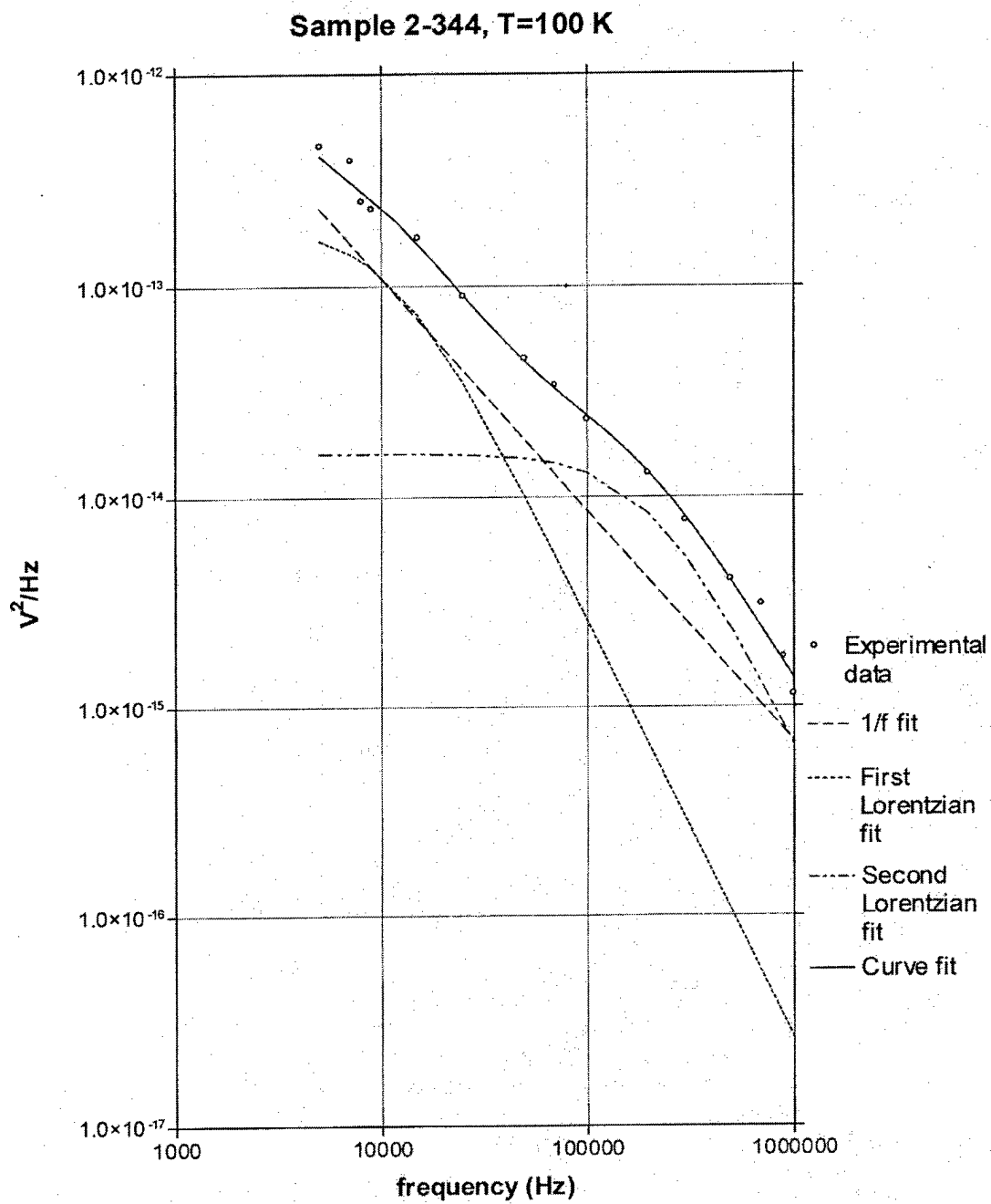


Figure 8.

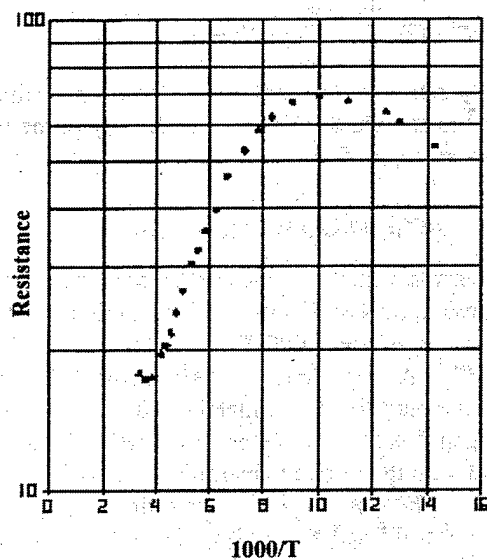


Figure 9. Resistance vs. $1000/T$ for sample 2-348.

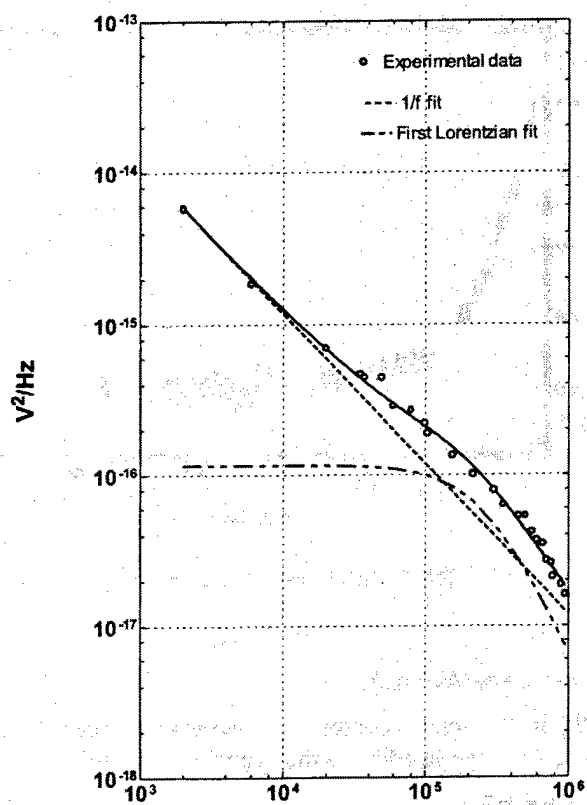


Figure 10. Spectral density $S_v(f)$, sample 2-348, $T=300\text{K}$.

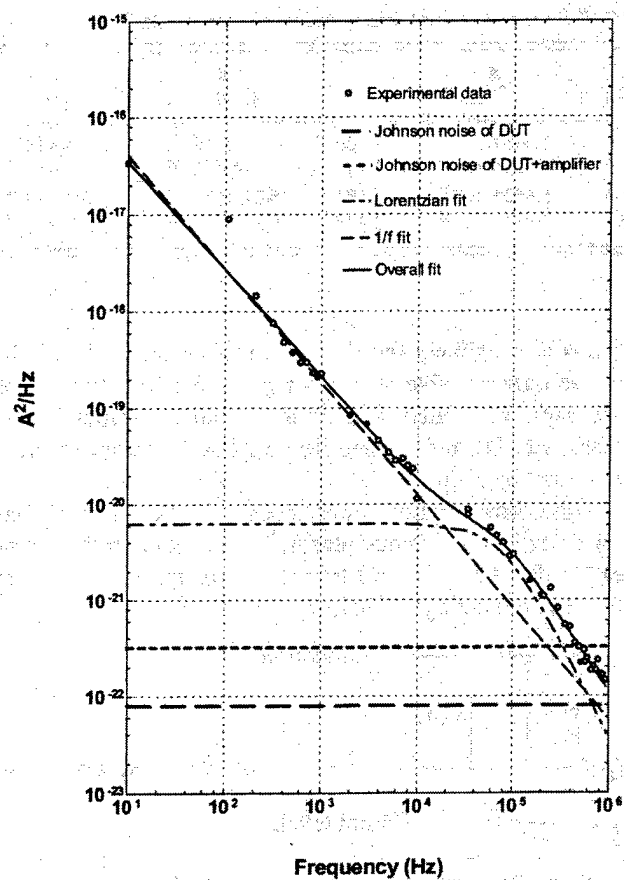


Figure 11. Spectral density $S_I(f)$, sample 2-348, $T=100\text{K}$.

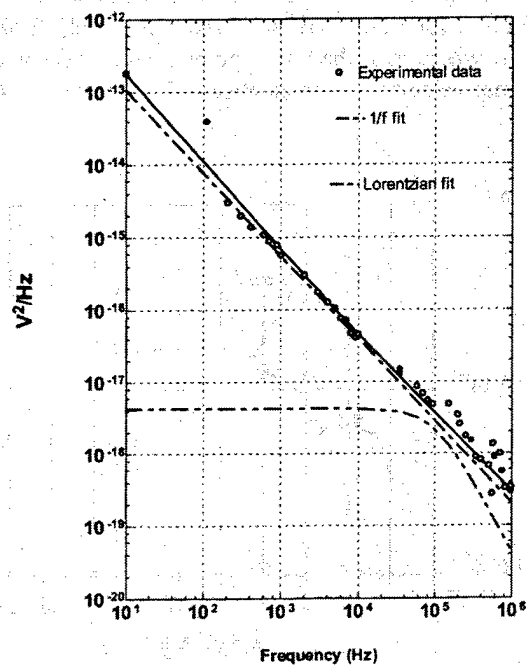


Figure 12. Spectral density $S_I(f)$, sample 2-348, $T = 50\text{K}$.

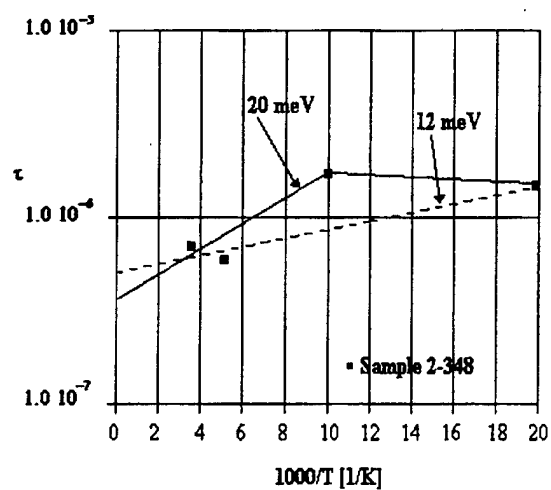


Figure 13. Log (lifetime) vs. $1000/T$, sample 2-348.